Robust Interpolating Traffic Signal Control for Uncertain Road Networks

Shimon Komarovsky and Jack Haddad*

Abstract— **Many traffic control strategies in the literature are designed based on various traffic flow models, which do not include parameter uncertainties in their intersection flow dynamics. Hence, these control strategies are unable to handle conditions when the assumed values for the parameters vary significantly from their real values. Moreover, many utilized state feedback control approaches to develop the traffic signal controllers lack the treatment of control and state constraints directly in the design phase.**

This paper considers robust traffic signal control for uncertain urban road networks. First, parameter uncertainties are integrated into the store-and-forward (SF) model, which is utilized in this paper to describe the flow dynamics for traffic signalized intersections. Then, the uncertain SF model is utilized to design a robust feedback controller by an interpolation-based approach. This approach (i) guarantees robustness against all parameter uncertainties, (ii) handle control and state constraints, and (iii) present a computationally cheap solution. Finally, numerical results for an isolated signalized intersection show a comparison between the developed interpolating controllers and other controllers in the literature. The results demonstrate the performance advantages from applying the robust interpolating controllers.

I. Introduction

Mitigating congestion in urban road networks still remains as one of the current great challenges in traffic control. To address the traffic congestion, many model-based control strategies have been developed for urban traffic networks during the past few decades, see e.g. [1].

The Store-and-Forward (SF) model is one of the most prominent models in the literature [2], as several variants have been introduced, and many traffic control strategies have been designed based on these variants [2]–[7].

The core modeling idea of the SF is introducing a model simplification that enables the mathematical description of the traffic flow process at signal light without the use of discrete variables. In other words, the SF model disregards the inner dynamics within a cycle of green phase and then red phase. On one hand, the latter might reduce the model accuracy, while on the other hand, it can result in a simplified model that can be utilized for control design.

This model simplification enables the application of a number of highly efficient optimization and control methods, such as linear programming (LP), quadratic programming (QP), etc. However, most traffic control strategies have been designed based on traffic flow models, which do not include parameter uncertainties in their intersection flow dynamics, and only a few variants deal explicitly with model uncertainties. The parameter uncertainties may include the saturation flow rates, turning movement rates, and others, that are difficult to estimate in reality. The model parameters are assumed to be a priori known or estimated. Hence, the resulted control strategies are unable to handle conditions when the assumed values for the parameters vary significantly from their real values, e.g. applying variants of linear quadratic regulator (LQR) on uncertain traffic model might cause low control performances, as they cannot compensate parameter uncertainties.

Moreover, many feedback control approaches which are utilized to develop the traffic signal controllers lack the treatment of control and state constraints directly in the design phase.

Recent robust control methods were proposed to consider traffic uncertainties in traffic signal control problems [3]–[6]. Robust control deals with unknown but bounded model parameters, as it optimizes an objective function and/or operates under control specifications when worst case scenarios are taken into account. Indeed, robust control can compensate the parameter uncertainties, and it can be very effective for systems with structured parameter variations [8], however, robust control usually results in a conservative design.

In this paper, an uncertain SF model is first developed. The uncertain SF model is then utilized to design a robust feedback controller by an interpolation-based approach [9]. The theory of interpolation-based control was recently developed in [10] and [11], while recently was implemented for traffic perimeter control problems, e.g. [12], and was applied in lab experiments of vehicle platoon formation in [13]. The results in these previous works encourage us to study the interpolation-based control on the traffic signal control problem. The interpolation-based approach (i) guarantees robustness against all parameter uncertainties, (ii) handle control and state constraints, and (iii) present a computationally cheap solution. Two variants of interpolation-based control methods, i.e. Interpolating Control (IC) and Simple Interpolating Control (SIC), are applied.

Finally, considering an isolated signalized intersection, a comparison between the developed interpolating controllers and other controllers in the literature is conducted. The results demonstrate the performance advantages from applying the robust interpolating controllers.

II. Uncertain store-and-forward model for urban road networks

A. Store-and-forward dynamic equations

The store-and-forward dynamic equations are briefly introduced here following the description in [2], [14].

Let us consider an urban network which comprises several streets that cross at signalized intersections, $j \in J$, and

Shimon Komarovsky and Jack Haddad are with the Technion Sustainable Mobility and Robust Transportation (T-SMART) Laboratory, Technion–Israel Institute of Technology. * Corresponding author: jh@technion.ac.il

links (approaches) $z \in Z$. For each signalized intersection j, I_j and O_j denote the sets of incoming and outgoing links, respectively. It is assumed that the offset, the cycle time C_j, and the total lost time L_j of intersection j are fixed; for simplicity, $C_j = C$ is assumed for all intersections $j \in J$. Furthermore, the signal control of intersection j is based on a fixed number of stages that belong to the set F_j, while v_z denotes the set of stages where link z has a right-of-way. Finally, the saturation flows S_z, $z \in I_j$, and the turning movement rates $t_{z,w}$, $z \in I_j$, $w \in O_j$, are assumed known and fixed.

The link outflow is a discrete-event process with two periods, i.e. green light $[0, G_z)$ and red light $[G_z, C]$. The outflow is assumed to be equal to the maximum flow value, i.e. the saturation flow S_z, during the whole or part of the green light for oversaturated or undersaturated condition, respectively, while during the red light the outflow is equal to zero. However, to simplify the modeling complexity, instead of modeling two levels of value for the outflow during a cycle, the SF model describes the average outflow per second over the cycle time. The averaged outflow for link z at cycle k, i.e. $u_z(k)$, and calculated as follows:

$$u_z(k) = S_z G_z(k)/C\,, \tag{1}$$

where $G_z(k)$ [s] is the effective green duration of link z at cycle k, calculated as $G_z(k) = \sum_{i \in v_z} g_{j,i}(k)$, where $g_{j,i}(k)$ is the green duration of stage i at intersection j at cycle k.

Hence, for each link (approach) $z \in Z$, the vehicle conservation equation can be written as, see also Fig. 1,

$$x_z(k+1) = x_z(k) + T[q_z(k) - s_z(k) + d_z(k) - u_z(k)], \tag{2}$$

where $x_z(k)$ [veh] is the number of vehicles (or sometimes is referred as queue in the following) within link z at the beginning of cycle k, $d_z(k)$ [veh/s] and $s_z(k)$ [veh/s] are the traffic flow demand and the exit flow, respectively, and $q_z(k)$ and $u_z(k)$ are respectively the average inflow and outflow of link z over the period $[kT, (k+1)T]$, where T is the control interval (cycle time duration) and k is the cycle time index $k = 1, 2, \ldots K$. Following [14], the inflow to the link z is

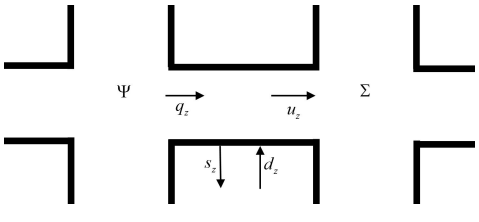

Fig. 1. A schematic road link (based on [2]).

given by $q_z(k) = \sum_{w \in I_\Psi} t_{w,z} u_w(k)$, where $t_{w,z}$ with $w \in I_\Psi$ are the turning rates towards link z from the links that enter intersection Ψ. The exit flow $s_z(k)$ is determined by $s_z(k) = t_{z,0} q_z(k)$, where the exit rates $t_{z,0}$ are assumed to be known and constant.

Now, substituting the above equations for inflow and exit flows and (1) into (2) for all z, then replacing the variable from $G_z(k)$ to $g_{j,i}(k)$, and finally organizing all resulting equations in one single vector-based equation leads to the following linear state-space form

$$\mathbf{x}(k+1) = A\mathbf{x}(k) + B\mathbf{g}(k) + T\mathbf{d}(k)\,, \tag{3}$$

where the state vector $\mathbf{x}(k)$ consists the number of vehicles x_z for all links, the control vector $\mathbf{g}(k)$ consists of the green times $g_{j,i}$ for all stages, and the disturbance vector $\mathbf{d}(k)$ consists of the demand flows d_z of each link z. The matrix B is a constant matrix of appropriate dimensions containing the network characteristics, i.e. topology, saturation flows, and turning rates.

Note that the model (3) can be rewritten as a linear model with deviation state variables around an equilibrium point $(\mathbf{x}^{\mathrm{N}}, \mathbf{g}^{\mathrm{N}}, \mathbf{d}^{\mathrm{N}})$. It would be more reasonable to regulate the dynamic system around an equilibrium point, which is not equal to zero, but corresponds to nominal queue lengths and green durations.

Therefore, the corresponding linear model for deviation variables is of the form

$$\Delta\mathbf{x}(k+1) = A\Delta\mathbf{x}(k) + B\Delta\mathbf{g}(k) + T\Delta\mathbf{d}(k), \tag{4}$$

where $\Delta\mathbf{x}(k) = \mathbf{x}(k) - \mathbf{x}^{\mathrm{N}}$, $\Delta\mathbf{g}(k) = \mathbf{g}(k) - \mathbf{g}^{\mathrm{N}}$, $\Delta\mathbf{d} = \mathbf{d}(k) - \mathbf{d}^{\mathrm{N}}$. $\mathbf{x}^{\mathrm{N}}$ is free to choose, however, $\mathbf{g}^{\mathrm{N}}$ and $\mathbf{d}^{\mathrm{N}}$ are functionally dependent. Substituting nominal values in the conservation formula (3), i.e. $\mathbf{g}(k) = \mathbf{g}^{\mathrm{N}}$, $\mathbf{d}(k) = \mathbf{d}^{\mathrm{N}}$, $\mathbf{x}(k+1) = \mathbf{x}(k) = \mathbf{x}^{\mathrm{N}}$, and $A = I$ according to (3),

$$B\mathbf{g}^{\mathrm{N}} + T\mathbf{d}^{\mathrm{N}} = 0\,. \tag{5}$$

Note that it is usually assumed that the deviation in demand is equal to zero for control design, i.e. $\Delta\mathbf{d}(k) = 0$ or in other words the demand stays constant and equal to $\mathbf{d}^{\mathrm{N}}$. Hence, eventually (4) becomes

$$\Delta\mathbf{x}(k+1) = A\Delta\mathbf{x}(k) + B\Delta\mathbf{g}(k). \tag{6}$$

B. Modeling uncertainty in the SF model

Urban road networks in reality include many uncertainties. Therefore, in relation to our problem formulation, some of the parameters that characterize the network should be assumed as uncertain parameters. The SF model utilizes the following parameters for each link in a network:

- Saturation flows vector S_z [veh/h], which influences the outflow $u_z(t)$ [veh/h],
- Turning rates (matrix) $t_{w,z}$ [veh/h] towards link z from other links w, which influence the inflow $q_z(t)$ [veh/h],
- Exit rates vector $t_{z,0}$ [veh/h], which influences the exit flows $s_z(k)$ [veh/h].

In previous works, all above parameters are assumed ideally to be fixed and known, but in reality they are uncertain parameters that might be unknown and/or changing over time. The parameter uncertainties would affect only the B matrix, and eventually the control performances as they are not designed to compensate uncertainties. The parameter uncertainties are integrated in the SF model by introducing uncertainty sets. It is assumed that the saturation flow S_z, the turning rate $t_{w,z}$, and the exit rate $t_{z,0}$ of link $z \in Z$, belong to interval sets.

C. Traffic flow constraints at signalized intersections

State and control constraints are imposed on each link and individual isolated intersection in the network, [2].

1) State constraints: Queue lengths are subject to lower and upper bound constraints, i.e.

$$0 \leq x_z \leq x_z^{\max} \qquad \forall z \in Z, \tag{7}$$

where $x_z^{\max}$ is the maximum admissible queue length.

2) Control constraints:

$$\sum_{i \in F_j} g_{j,i} + L_j = (\text{or} \leq) C \tag{8}$$

must hold at each intersection j, where $g_{j,i}$ is the green time of stage i at intersection j. Another control constraints are given as follows

$$g_{j,i,\min} \leq g_{j,i} \leq g_{j,i,\max}, \tag{9}$$

which are the upper and lower bound constraints, i.e. the green light durations are in some minimum-maximum ranges.

Following the linear model for deviation variables, see (4), the state constraints (7) and the control constraints (9) can be re-written respectively as

$$-x_z^{\mathrm{N}} < \Delta x_z < x_z^{\max} - x_z^{\mathrm{N}}\,, \tag{10}$$

$$g_{j,i,\min} - g_{j,i}^{\mathrm{N}} \leq \Delta g_{j,i} \leq g_{j,i,\max} - g_{j,i}^{\mathrm{N}}\,, \tag{11}$$

and if the sum of green duration constraints equation (8) is subtracted from the same equation (8) applied to nominal values $\sum_{i \in F_j} g_{j,i}^{\mathrm{N}} + L_j = C$, then one gets

$$\sum_{i \in F_j} \Delta g_{j,i} = (\text{or} \leq) 0\,. \tag{12}$$

Note that the constraints (12) will hold with equality during (over)saturated conditions, while during undersaturated conditions the inequality of the constraints will hold.

III. Interpolation-based control for traffic signals

Interpolating Control (IC) [10] is a regulating control method, which can handle model uncertainties and allow inclusion of state and control constraints. It also guarantees recursive feasibility and asymptotic stability, for all feasible initial conditions. Recently, a new simple version of IC, using saturated control inputs and ellipsoidal feasible sets, called Simple Interpolating Control (SIC) was presented in [15]. Unlike IC, SIC does not need to solve an LP at each time step, which is less computationally expensive than IC.

In this paper, IC and SIC methods will be implemented to design traffic signal control. Both methods can handle uncertain and/or time-varying linear discrete time systems, i.e. they can be utilized to design robust traffic signal controllers.

Both interpolation-based design methods can be seen as alternatives to optimization-based control schemes such as Model Predictive Control. The design methods are suitable for problems which finding the optimal solution requires calculations, where IC and SIC can provide straightforward suboptimal solutions. In the following sections, a summary of the methods proposed in [9], [10], [15], [16] is presented.

A. Interpolating Control (IC) formulation

Let us consider the following uncertain and/or time-varying linear discrete-time system:

$$\Delta \mathbf{x}(k+1) = A(k)\Delta \mathbf{x}(k) + B(k)\Delta \mathbf{g}(k)\,, \tag{13}$$

where $\Delta \mathbf{x}(k) \in \mathbb{R}^n$ is the state and $\Delta \mathbf{g}(k) \in \mathbb{R}^m$ is the control input. The matrices $A(k) \in \mathbb{R}^{n \times n}$ and $B(k) \in \mathbb{R}^{n \times m}$ are given with polytopic uncertainty as follows

$$A(k) = \sum_{i=1}^{s} \alpha_i(k) A_i, \qquad B(k) = \sum_{i=1}^{s} \alpha_i(k) B_i, \tag{14a}$$

$$\sum_{i=1}^{s} \alpha_i(k) = 1,\ \alpha_i(k) \geq 0,\ \forall i = 1, \ldots, s, \tag{14b}$$

where $\alpha_i(k)$ is unknown and time-varying. The state and the control are subject to the following polytopic constraints:

$$\Delta \mathbf{x}(k) \in \mathcal{X} = \{\Delta \mathbf{x} \in \mathbb{R}^n : F_x \cdot \Delta \mathbf{x}(k) \leq g_x\}, \tag{15a}$$

$$\Delta \mathbf{g}(k) \in \mathcal{U} = \{\Delta \mathbf{g} \in \mathbb{R}^m : F_u \cdot \Delta \mathbf{g}(k) \leq g_u\}, \tag{15b}$$

where $F_x \in \mathbb{R}^{n_{g_x} \times n}, F_u \in \mathbb{R}^{n_{g_u} \times m}$ with n_{g_x}, n_{g_u} as the number of half-spaces defining state and control constraints, respectively.

Assuming a robustly stabilizing control law, such as

$$\Delta \mathbf{g}_0(k) = L \Delta \mathbf{x}(k), \tag{16}$$

while imposing input and state constraints with L as some given gain matrix, one can calculate $\Omega_{\max}$, a *maximal admissible invariant set* (MAS) for which any starting point inside the set will converge to the origin according to the control law (16). Afterwards, one can calculate C_N, a *controlled invariant set* for some specific size of a receding window, i.e. a set of states for which there exists an admissible control sequence such that states starting in it, will be steered into $\Omega_{\max}$ in no more than N steps. Obviously $\Omega_{\max} \subset C_N$. The $\Omega_{\max}$ is the inner set and designed for performance (16), while C_N is the outer set and designed to enlarge the admissible set.

An outer vertex control $\Delta \mathbf{g}_\nu$, refer to [10] for more details, can be fully exploited only on the border of C_N. Note that the time to regulate the plant state to the origin would be much longer compared to the inner controller, i.e a more aggressive local controller $\Delta \mathbf{g}_0(k)$ operating near the origin in $\Omega_{\max}$. Therefore, it is preferable that the control for an initial state in the outer region should be eventually switched to the inner controller. The outer and inner controllers are interpolated by applying a convex combination as follows,

$$\Delta \mathbf{g}(k) = c(k)\Delta \mathbf{g}_\nu(k) + (1 - c(k))\Delta \mathbf{g}_0(k)\,, \tag{17}$$

where $0 \leq c(k) \leq 1$ is the interpolating coefficient, which is minimized in order to have the state as close as possible to the $\Omega_{\max}$, implying a better control performance. The interpolating coefficient is calculated by solving an LP. The inner controller Δg_0 is assumed to be chosen a priori, e.g. (16), and the outer controller can be found by solving an LP each sample step. Hence, at each time step, two LPs should be solved. For a detailed information, the reader can refer to [10].

B. Simple Interpolating Control (SIC)

Compared to IC, the SIC method brings simpler algorithms, which provide a good compromise between computational load, feasible region, and performance.

The SIC method relies on two saturating linear control laws of the form $\Delta\mathbf{g}(k) = \text{sat}(L\Delta\mathbf{x}(k))$, and two robustly contractive ellipsoids, replacing the polyhedrons in IC, associated to these control laws. The outer controller, $\Delta\mathbf{g}_b(k) = \text{sat}(L_b\Delta\mathbf{x}(k))$, maximizes the invariant set for possible states, where its gain matrix L_b is calculated by solving a formulated LMI problem, refer to [9]. While the inner controller, $\Delta\mathbf{g}_a(k) = \text{sat}(L_a\Delta\mathbf{x}(k))$, is responsible for a high performance, where its gain matrix L_a is calculated in advance from solving the Riccati equation of an LQR problem.

The ellipsoids are determined by positive definite matrices P_a and P_b, as $\mathcal{E}(P_i) = \{\Delta\mathbf{x} : \Delta\mathbf{x}^\top P_i^{-1}\Delta\mathbf{x} \leq 1\}$, where $i = a, b$. The constraints are assumed to be symmetric around the origin and represented by polytopes of the form:

$$\Delta\mathbf{x}(k) \in \mathcal{X} = \{\Delta\mathbf{x} \in \mathbb{R}^n : \|F \cdot \Delta\mathbf{x}(k)\|_\infty \leq 1\}, \quad (18a)$$

$$\Delta\mathbf{g}(k) \in \mathcal{U} = \{\Delta\mathbf{g} \in \mathbb{R}^m : \|\Delta\mathbf{g}(k)\|_\infty \leq \Delta\mathbf{g}_{\max}\}, \quad (18b)$$

where $F \in \mathbb{R}^{n_c \times n}$ and $\Delta\mathbf{g}_{\max} = \min(g^{\text{N}}_{j,i} - g_{j,i,\min}, g_{j,i,\max} - g^{\text{N}}_{j,i}) \in \mathbb{R}^m$.

Finally, the inner and outer controllers are blended, similarly to (17), as

$$\Delta\mathbf{g}(k) = c(k)\text{sat}(L_b\Delta\mathbf{x}_b(k)) + (1 - c(k))\text{sat}(L_a\Delta\mathbf{x}_a(k)), \quad (19)$$

where $0 \leq c(k) \leq 1$ and at each step $\Delta\mathbf{x}_b(k)$, $\Delta\mathbf{x}_a(k)$, $c(k)$ are calculated simply algebraically without any LP problem to solve, see equations (7)–(9) in [15].

IV. Numerical Examples

The performance of the interpolating controllers is examined via an application of traffic signal control for an isolated signalized intersection. The intersection has two movements/states, and two phases/controllers.

Two numerical examples are presented: example 1 deals with a nominal case scenario, while example 2 deals with an uncertain case scenario. In example 1, comparison is carried out between the results obtained from applying the interpolating controllers and another two controllers, designed by well-known and established methods in the literature: Linear Quadratic Regulator (LQR) and MPC controller. Both controllers are designed with the objective to regulate the plant state to the origin. Because of space limitation, the LQR and MPC control design for the isolated signalized intersection based on the SF model is not presented here. The reader can refer to [14] and [7] for the LQR and MPC, respectively.

A. Numerical example 1: Nominal case

First, a sensitivity analysis is carried out to study how changing the constraints (10) and (11) influences the invariant sets $\Omega_{\max}$, C_N, and the trajectories.

The effect of changing the relative values of $x_1^{\max}$ and $x_2^{\max}$ in (10) on the $\Omega_{\max}$ is shown in Fig. 2(a). It is shown that changing the relative values of $x_1^{\max}$ and $x_2^{\max}$ changes the shape of the $\Omega_{\max}$ in different directions. Note that the constraint (12) is shown in the figure as a red line.

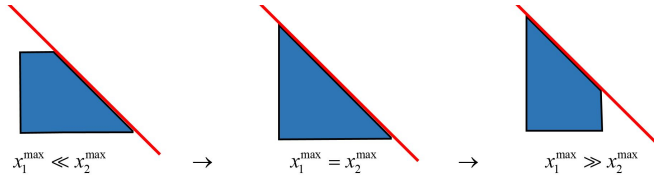

(a) Changing the relative values of $x_1^{\max}$, $x_2^{\max}$ in (10).

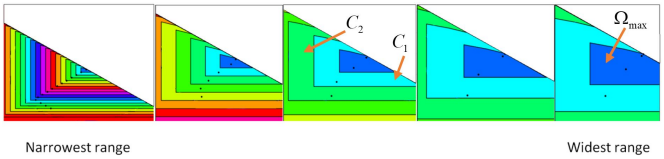

(b) Changing the limits of the constraint (11) by $g_{j,i,\min}$ and $g_{j,i,\max}$.

Fig. 2. Example 1: The effect of the constraints (10) and (11) on the invariant sets $\Omega_{\max}$, C_N, and the trajectories.

The effects of changing the values of $g_{j,i,\min}$ and $g_{j,i,\max}$ in (11) on the $\Omega_{\max}$, C_N, and trajectories are shown in Fig. 2(b). It is shown that relaxing the limits of constraint (11), i.e. widening the control feasible set, results in a larger $\Omega_{\max}$ region, and accordingly a larger C_N. The black dots in each subfigure show a trajectory that starts from an initial state and ends at the origin. Comparing the trajectories of narrow and wide ranges, it is also shown that less number of control steps is needed to reach the origin for wide ranges. It should be stressed that a wider range means less constrictive process, which implies a larger $\Omega_{\max}$, and as a result a larger control admissible region is obtained at each step, which in its turn allows a faster convergence to the origin via less steps. The results for IC trajectories from different initial states, for the case of $x_1^{\max} = x_2^{\max}$, are shown in Fig. 3.

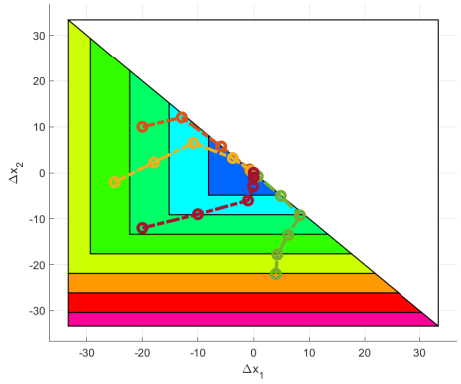

Fig. 3. Example 1: IC trajectories from different initial states.

Trajectories and control inputs over time results, i.e. $\Delta x_1(t)$, $\Delta x_2(t)$ and $\Delta g_1(t)$, $\Delta g_2(t)$, are shown in Fig. 4 for (i) IC, (ii) SIC, (iii) MPC, and (iv) LQR. All methods take into account the constraints (10)–(12). Note that the implemented LQR takes into account the constraints by imposing them after control input calculations.

The results show that the MPC and LQR controllers con-

verge faster to the origin compared with the IC and SIC. Actually, the MPC, when it is unconstrained, has identical optimal solution to the LQR, given the same objective function. Note that SIC with constraints converges even slower than the IC, probably because of the constraint symmetry requirements of the method, see (18), which render the SIC to be more conservative than IC.

Indeed, the IC and SIC might provide sub-optimal solutions in terms of convergence, however, the IC and SIC controllers have advantages over the MPC and LQR controllers in the context of computational complexity, which will be considered in the following subsection.

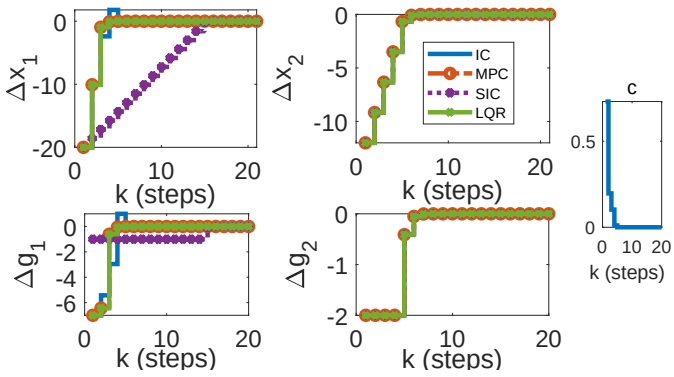

Fig. 4. Example 1: Trajectories and control inputs over time results obtained from (i) IC, (ii) SIC, (iii) MPC, and (iv) LQR.

B. Computational efforts analysis

The computation effort of the controller is an important comparison criteria. Previous analysis of the computational efforts for the IC controller, and comparison with MPC and LQR controllers, have been conducted in [10], [13]. These works present the computational advantage of IC controllers over MPC and LQR controllers.

In the following, we conduct a further comparison oriented to our the traffic control problem dealt with in this paper. We would like to compare some complexity characteristics, in order to evaluate the tradeoff between performance, presented in the previous subsection, and computation load/time.

The computational efforts are compared by examining the number of constraint equations and the number of variables in the problems of the LQR, MPC, IC, and SIC methods. The results of this analysis are summarized in Table I, where the notations are as follows: *dlqr* is the discrete-time Riccati equation solver, *LMI* is the linear matrix inequalities, *LP* is the Linear Programming, *QP* is the Quadratic Programming, *nx* is the total number of states, *nu* is the total number of controls (total phases in all intersections), *njuncs* is the number of intersections, N_{p} is the MPC prediction and control horizon, *ngi* and *ngo* are the number of half-planes defining the sets $\Omega_{\max}$ and C_N, respectively, see [9]. Note that the QP is imposed on the LQR at each time step, while it is imposed on the SIC only if needed, i.e. when the (12) is violated.

It is noticeable from Table I that the IC and SIC methods generate significantly smaller problems than the LQR and MPC, which are beneficial in real-time computing applications. The performance of the IC and SIC controllers, on the other hand, are only slightly decreased compared to the MPC, as shown in the previous subsection.

TABLE I

COMPLEXITY COMPARISON TABLE.

Feature	LQR	MPC	IC	SIC
offline solver	dlqr	–	$\Omega_{\max}$, C_N computation	2·(2nu+nx) LMI's
online solver 1	QP	QP	LP	QP (if needed)
# of constraints	njuncs	nx $\cdot N_{\mathrm{p}}$	ngo+ngi	njuncs
# of variables	nu	nu$\cdot N_{\mathrm{p}}$	nx+1	nu
online solver 2	–	–	LP	–
# of constraints	–	–	ngo+2nu+1	–
# of variables	–	–	nu+1	–

C. Numerical example 2: Robust case

As mentioned in Section II, several uncertainties might exist in the urban road networks. In this numerical example, uncertainty in saturation flows will be considered.

To evaluate the performance of robust IC controllers, we compare between a robust IC controller and an IC controller designed for nominal conditions, i.e. when we design the IC controller, the values of the saturation flow S_z are assumed to be equal to the middle of the uncertain range of S_z. However, the saturation values in the system plant, i.e. the reality, are uncertain which can randomly vary within the uncertain saturation set, determined by the parameter $\alpha(t)$, see (14).

The effect of uncertainty on the invariant sets $\Omega_{\max}$ and C_N is shown in Fig. 5(a). As the uncertainty in saturation flows increases, i.e. increasing the range of the uncertain saturation set, the invariant sets $\Omega_{\max}$, C_N become smaller. I.e. larger uncertainties in S_z imply smaller state set for feasible initial queue lengths at the intersection that can be steered to equilibrium queue lengths.

Fig. 5(b) shows the trajectory results $\Delta x_1(t)$ and $\Delta x_2(t)$ for a nominal controller, and robust controllers designed for different sizes of uncertainty set, applied to an uncertain plant which its saturation flows S_z change randomly according to $\alpha(t)$ in the figure. The results show that all controllers succeed to bring the initial queue lengths to the equilibrium lengths even under uncertainties in saturation flows. The results in Fig. 5(b) also show that the nominal IC controller can perform well under the uncertainty compared with the robust controllers, in terms of reaching equilibrium in faster times.

To explore further this observation, for a fixed given size of uncertainty set, we compare the performance results of a nominal IC controller with a robust IC controller, designed accordingly to the given uncertainty set, for three different fixed plant uncertainties, $\alpha = 0.2, 0.5, 0.9$, see Fig. 6. The trajectories obtained from applying the nominal controller converge to the origin faster than the robust controllers. The robust controllers seem to be more conservative and cautious not to violate the constraints in expense of faster convergence.

In spite of the well performance of the nominal IC controllers indicated above, i.e. in Fig. 5(b) and Fig. 6, the results in Fig. 7 demonstrate the importance of designing robust controllers. In Fig. 7, the nominal IC controllers are run for the case without plant uncertainty, and the cases with $\alpha(t) = 0.2, 0.9$.

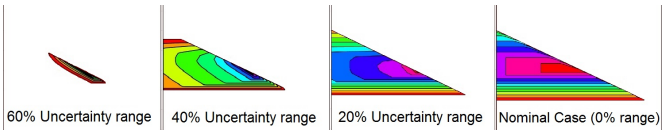

(a) Invariant sets for different sizes of uncertainty set.

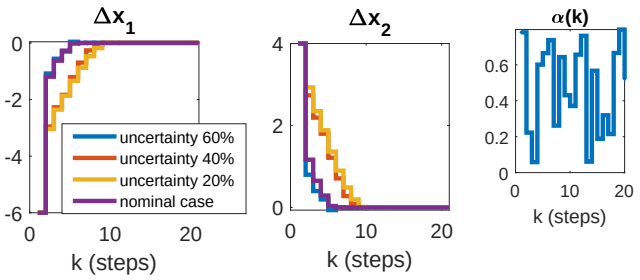

(b) State evolutions for different sizes of uncertainties.

Fig. 5. Example 2: Effects of different sizes of saturation flow uncertainties.

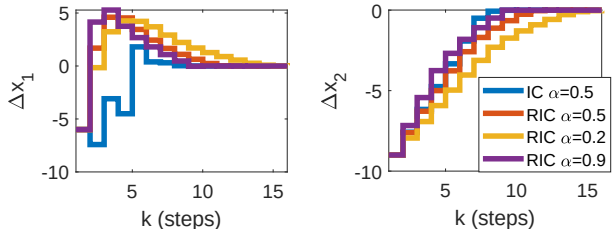

Fig. 6. Example 2: Nominal vs. robust IC state evolutions for different fixed plant uncertainties under saturation flows uncertain set..

As expected and shown in the figure, the nominal controller might fail in bringing the initial state to the the equilibrium state when it is applied for an uncertain plant, e.g. with $\alpha = 0.9$. Such a failure situation would not have happened if a robust controller was applied.

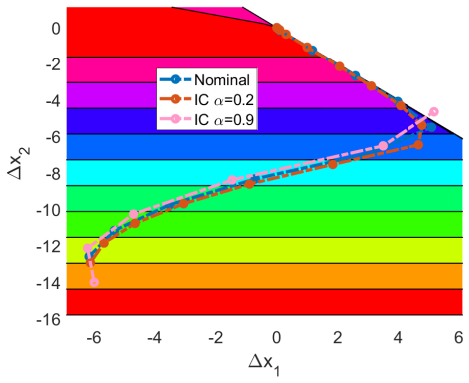

Fig. 7. Example 2: Nominal trajectories under different fixed plant uncertainties under saturation flows uncertain set.

V. Conclusions and Future Work

In this paper, an uncertain store-and-forward model has been developed as parameter uncertainties were integrated in the traffic flow dynamics for signalized intersections. The developed IC and SIC controllers guarantee robustness against all parameter uncertainties, treat control and state constraints directly in the design phase, and present computationally cheap solutions. As far as the authors know, this is the first time that the interpolation-based approach is explored to design traffic control for signalized intersections. Comparison of numerical results between the developed interpolating controllers and other controllers in the literature for an isolated signalized intersection demonstrate the performance advantages from applying the robust interpolating controllers.

Scalability analysis of implementing the traffic interpolating controllers to large-scale urban networks should be studied. The current paper focused on investigating the effect of saturation flow uncertainty. Future research will be dedicated to study other parameter uncertainties.

References

[1] M. Papageorgiou, C. Diakaki, V. Dinopoulou, A. Kotsialos, and Y. Wang, "Review of road traffic control strategies," *Proceedings of the IEEE*, vol. 91, no. 12, pp. 2043–2067, 2003.

[2] K. Aboudolas, M. Papageorgiou, and E. Kosmatopoulos, "Store-and-forward based methods for the signal control problem in large-scale congested urban road networks," *Transportation Research Part C: Emerging Technologies*, vol. 17, no. 2, pp. 163–174, 2009.

[3] Y. Yin, "Robust optimal traffic signal timing," *Transportation Research Part B: Methodological*, vol. 42, no. 10, pp. 911–924, 2008.

[4] S. V. Ukkusuri, G. Ramadurai, and G. Patil, "A robust transportation signal control problem accounting for traffic dynamics," *Computers & Operations Research*, vol. 37, no. 5, pp. 869–879, 2010.

[5] T. Tettamanti, T. Luspay, B. Kulcsar, T. Peni, and I. Varga, "Robust control for urban road traffic networks," *IEEE Transactions on Intelligent Transportation Systems*, vol. 15, no. 1, pp. 385–398, 2014.

[6] L. Zhang, Y. Yin, and Y. Lou, "Robust signal timing for arterials under day-to-day demand variations," *Transportation Research Record: Journal of the Transportation Research Board*, no. 2192, pp. 156–166, 2010.

[7] K. Aboudolas, M. Papageorgiou, A. Kouvelas, and E. Kosmatopoulos, "A rolling-horizon quadratic-programming approach to the signal control problem in large-scale congested urban road networks," *Transportation Research Part C: Emerging Technologies*, vol. 18, no. 5, pp. 680–694, 2010.

[8] K. J. Astrom and B. Wittenmark, *Adaptive control*. Courier Corporation, 2013.

[9] H.-N. Nguyen, "Constrained control of uncertain, time-varying, discrete-time systems," *An Interpolation-Based Approach (Cham: Springer)*, 2014.

[10] H.-N. Nguyen, P.-O. Gutman, S. Olaru, and M. Hovd, "Implicit improved vertex control for uncertain, time-varying linear discrete-time systems with state and control constraints," *Automatica*, vol. 49, no. 9, pp. 2754–2759, 2013.

[11] H.-N. Nguyen, P.-O. Gutman, and R. Bourdais, "More efficient interpolating control," in *Control Conference (ECC), 2014 European*. IEEE, 2014, pp. 2158–2163.

[12] J. Haddad, "Robust constrained control of uncertain macroscopic fundamental diagram networks," *Transportation Research Part C: Emerging Technologies*, vol. 59, pp. 323–339, 2015.

[13] A. Tuchner and J. Haddad, "Vehicle platoon formation using interpolating control: A laboratory experimental analysis," *Transportation Research Part C: Emerging Technologies*, vol. 84, pp. 21–47, 2017.

[14] C. Diakaki, M. Papageorgiou, and K. Aboudolas, "A multivariable regulator approach to traffic-responsive network-wide signal control," *Control Engineering Practice*, vol. 10, no. 2, pp. 183–195, 2002.

[15] P. Mercader, D. Rubin, H.-N. Nguyen, A. Bemporad, and P.-O. Gutman, "Simple interpolating control," in *9th IFAC Symposium on Robust Control Design (ROCOND'18) and 2nd IFAC Workshop on Linear Parameter Varying Systems (LPVS'18)*, Florianopolis, Brazil, September 3-5 2018.

[16] H. Nguyen, P.-O. Gutman, S. Olaru, M. Hovd, and F. Colledani, "Improved vertex control for time-varying and uncertain linear discrete-time systems with control and state constraints," in *American Control Conference (ACC), 2011*. IEEE, 2011, pp. 4386–4391.